arXiv:1611.10177v3 [nucl-th] 18 Jan 2017

QUASIFISSION DYNAMICS AND STABILITY OF SUPERHEAVY SYSTEMS*

Kazuyuki Sekizawa[1] and Sophia Heinz[2,3]

[1]Faculty of Physics, Warsaw University of Technology, ulica Koszykowa 75, 00-662 Warsaw, Poland
[2]GSI Helmholtzzentrum für Schwerionenforschung GmbH, 64291 Darmstadt, Germany
[3]Justus-Liebig-Universität Gießen, II. Physikalisches Institut, 35392 Gießen, Germany

Recent experiments revealed intriguing similarities in the ^{64}Ni+^{207}Pb, ^{132}Xe+^{208}Pb, and ^{238}U+^{238}U reactions at energies around the Coulomb barrier. The experimental data indicate that for all systems substantial energy dissipation takes place, in the first stage of the reaction, although the number of transferred nucleons is small. On the other hand, in the second stage, a large number of nucleons are transferred with small friction and small consumption of time. To understand the observed behavior, various reactions were analyzed based on the microscopic time-dependent Hartree-Fock (TDHF) theory. From a systematic analysis for ^{40,48}Ca+^{124}Sn, ^{40}Ca+^{208}Pb, ^{40}Ar+^{208}Pb, ^{58}Ni+^{208}Pb, ^{64}Ni+^{238}U, ^{136}Xe+^{198}Pt, and ^{238}U+^{238}U reactions, we find that TDHF reproduces well the measured trends. In addition, the Balian-Vénéroni variational principle is applied to head-on collisions of ^{238}U+^{238}U, and the variance of the fragment masses is compared with the experimental data, showing significant improvement. The underlying reaction mechanisms and possible future studies are discussed.

PACS numbers: 25.70.-z, 25.70.Lm, 25.70.Hi, 25.85.-w, 21.60.Jz

1. Introduction

In heavy ion reactions at energies around the Coulomb barrier, a molecule-like nuclear system can be formed, which is called a nuclear molecule [1] or

* Based on discussion after a talk given by S. Heinz entitled *"Nuclear molecule formation and time delay in collisions of nuclei with $Z_1 + Z_2 \geq 110$"* presented at the XXIII Nuclear Physics Workshop „Marie & Pierre Curie", Kazimierz Dolny, Poland, September 27–October 2, 2016.

a dinuclear system [2], after mutual capture of projectile and target nuclei. At this stage, nucleons are exchanged actively and kinetic energy is dissipated, while the system evolves towards the equilibrium. Because of the strong Coulomb repulsion, the system can reseparate before compound nucleus (CN) formation (quasifission, QF), typically on the timescale of (10^{-21}–10^{-20}) sec, resulting in a characteristic correlation between fragment masses and scattering angles [3, 4, 5, 6, 7]. The QF process significantly hinders fusion of heavy nuclei leading to, *e.g.*, superheavy systems with proton numbers well beyond $Z = 100$, where the fragility of the composite systems is reflected by the small cross sections and short lifetimes of the fusion-evaporation residues.

The study of nuclear molecule formation and evolution allows to probe the stability of superheavy nuclear systems, also if they have proton numbers far beyond the ones of heaviest known elements. It is revealed by exit channel characteristics like mass, charge, angular and energy distributions. Binary reactions in the superheavy collision systems ^{64}Ni+^{207}Pb ($Z = Z_{\rm P} + Z_{\rm T} = 110$) [8] and ^{132}Xe+^{208}Pb ($Z = 136$) [9] were studied at the velocity filter SHIP at GSI. In both cases, clear signatures for the formation of long-lived nuclear molecules which rotate by large angles of 180 degrees were observed. Even in collisions of ^{238}U+^{238}U ($Z = 184$), which were investigated at the VAMOS spectrometer at GANIL [10], a noticeably large interaction time was deduced. A comparison of the behavior of energy dissipation, interaction times, and deformation reveals striking similarities between these three systems. To understand the underlying reaction mechanism is the main purpose of the present article.

To describe damped collisions of heavy nuclei, various models have been developed and applied: *e.g.* a dynamical model based on Langevin-type equations of motion [11, 12], a dinuclear system model (DNS) [13, 14, 15, 16], and an improved quantum molecular dynamics model (ImQMD) [17, 18, 19, 20]. Among those theoretical models, the time-dependent Hartree-Fock (TDHF) theory [21, 22] is regarded as a microscopic one which allows to investigate nuclear structure and reaction dynamics in a unified way from nucleonic degrees of freedom. Since a phenomenological input is only an energy density functional (EDF), which is constructed to reproduce known properties of finite nuclei and nuclear matter, it offers non-empirical predictions[1]. It has been shown that TDHF provides a fairly good description of averaged reaction outcomes, *e.g.*, mass and charge numbers of reaction products, total kinetic energy loss (TKEL) and scattering angle. Recent studies

[1] We note that although EDF dependence of TDHF results has not been well studied to date, and should be studied in future, QF dynamics (orientation dependence, shell effects, contact time, etc.) in, *e.g.*, the ^{64}Ni+^{238}U reaction with SLy5 in Ref. [23] and in the ^{48}Ca,^{50}Ti+^{249}Bk reactions with SLy4d in Ref. [24] shows very similar features.

demonstrated that the theory provides a reliable description also for deep-inelastic and QF processes in collisions of heavy nuclei [24, 25, 26, 27, 28, 29]. Here, we employ the TDHF theory to understand the experimental data.

The article is organized as follows. In Sec. 2, we outline the experimental methods of SHIP at GSI and VAMOS at GANIL. In Sec. 3, we recall the theoretical framework of TDHF. In Sec. 4, we present the experimental and theoretical results and discuss underlying reaction mechanisms. In Sec. 5, a summary and a perspective are given.

2. Experimental methods

In the following we briefly summarize our experimental methods. For detailed descriptions, we refer readers to Ref. [30] for the velocity filter SHIP at GSI and Ref. [31] for the VAMOS spectrometer at GANIL.

The experiments on ^{64}Ni+^{207}Pb and ^{132}Xe+^{208}Pb were performed at the velocity filter SHIP at GSI. We used SHIP to separate target-like transfer and QF products, emitted to forward angles of (0 ± 2) degrees, from primary beam and background events. The reaction products which passed SHIP were implanted in a position sensitive silicon strip detector where they were identified by α decay tagging. A large region of α emitters was populated in both experiments where we identified nuclei with $84 \leq Z \leq 89$. We measured velocity spectra for each isotope by scanning stepwise the electric and magnetic field values of SHIP and registering the yields of the identified nuclei at each setting. The velocity spectra deliver all essential information about formation and evolution of nuclear molecules, namely, about energy dissipation, lifetimes and rotation as well as on the deformation of the exit channel nuclei at the scission point.

The experiments on ^{238}U+^{238}U were performed at the VAMOS spectrometer at GANIL where we measured excitation functions of binary reaction products at five different beam energies around the Coulomb barrier. The reaction products were detected at angles of (35 ± 5) degrees. VAMOS was used in a pure quadrupole mode. The magnetic rigidity Bρ was optimized for the detection of transfer products with masses below uranium. The following detection system was used for particle identification and trajectory reconstruction: (i) a secondary electron detector for time-of-flight (TOF) measurements (start signal) and to trigger the data acquisition, (ii) two drift chambers for determining the positions (x, y) and scattering angles, (iii) an ionization chamber to measure the energy loss ΔE, (iv) a 500 μm thick Si wall to measure the residual energy and for TOF measurement (stop signal). From these parameters we obtained the mass number A and the proton number Z of the reaction products. The resolutions of A and Z were $\Delta A/A = 2\%$ (FWHM) and $\Delta Z/Z = 6\%$ (FWHM). The lowest accessible cross sections were about 1 μb.

3. Theoretical framework

In this section, we briefly recall the theoretical framework of the TDHF theory [21, 22]. In TDHF, the many-body wave function of the system is expressed as a single Slater determinant for all times,

$$\Phi(\boldsymbol{r}_1\sigma_1,\ldots,\boldsymbol{r}_N\sigma_N,t) = \frac{1}{\sqrt{N!}}\det\{\phi_i(\boldsymbol{r}_j\sigma_j q_j,t)\}, \tag{1}$$

where N $(= N_{\rm P} + N_{\rm T})$ is the total number of nucleons in the system, and $\phi_i(\boldsymbol{r}\sigma q,t)$ $(i = 1,\ldots,N)$ denotes the single-particle orbitals of the ith nucleon. $\boldsymbol{r}$, σ, and q are spatial, spin, and isospin coordinates, respectively. The Pauli exclusion principle is thus ensured during the entire time evolution. The time evolution of the single-particle orbitals is governed by the TDHF equations,

$$\mathrm{i}\hbar\frac{\partial\phi_i(\boldsymbol{r}\sigma q,t)}{\partial t} = \hat{h}(t)\phi_i(\boldsymbol{r}\sigma q,t), \tag{2}$$

where $\hat{h}(t)$ is the single-particle Hamiltonian which is dependent on single-particle orbitals at each time through various densities and is derived from appropriate functional derivatives of an EDF. The initial state for TDHF calculations is taken as a product of Slater determinants for Hartree-Fock (HF) ground states of projectile and target nuclei boosted with a relative velocity. The relative velocity is evaluated assuming the Rutherford trajectory. By solving the TDHF equations (2) with this initial wave function, the whole reaction dynamics, *e.g.*, energy dissipation, nucleon transfer, neck formation, QF or fusion, is described in real-space and real-time, from nucleonic degrees of freedom. We note that in TDHF calculations for heavy-ion reactions outlined above, neither adjustable parameters nor empirical assumptions on the dynamics are introduced.

4. Results and discussion

First, we show the experimental results for ^{64}Ni+^{207}Pb ($E_{\rm c.m.} = 289$ MeV), ^{132}Xe+^{208}Pb ($E_{\rm c.m.} = 492$ MeV), and ^{238}U+^{238}U ($E_{\rm c.m.} = 875$ MeV) reactions (Fig. 1). The lightest system, Ni + Pb, can still undergo fusion leading to isotopes of the element darmstadtium [32]. Therefore, one can expect signatures of formation of long-living nuclear molecules in this system. While the proton number of the composite system U + U is far beyond the one of the heaviest known elements and fusion reactions cannot be expected any more, it should give insight into the stability of the heaviest accessible systems. To probe the stability and time evolution of the composite nuclear systems, we investigate energy dissipation (*i.e.* TKEL), interaction times, and quadrupole deformation of the exit channel nuclei at the scission

point. The deformation was extracted assuming that the binary reaction products have the same quadrupole deformation and TKE is determined by the Coulomb potential at the scission point [9].

In Fig. 1, we show experimentally measured TKEL (a), interaction times (b), and quadrupole deformation (c) as a function of the fraction of transferred nucleons $\mathrm{d}A/A_{\mathrm{CN}}$, where A_{CN} denotes the total number of nucleons in the composite system. Figure 1 exhibits striking similarities between the different collision systems as well as between the different parameters (TKEL, interaction time, and deformation). Two stages of the reaction process are especially revealed by the behavior of TKEL and interaction times. The first stage ($\mathrm{d}A < 0.05A_{\mathrm{CN}}$) is characterized by a steep increase of these values, meaning that a large amount of energy is dissipated which consumes a lot of time but only a small number of nucleons are transferred. This is the transition regime from quasi-elastic to deep-inelastic reactions. After a net transfer of about 5% of the total number of nucleons in the composite system, the curves turn and approach a saturation value. In this second stage, the situation reverses and a large amount of nucleons can flow with small friction and small consumption of time.

It is striking that the slope change of TKEL and interaction times occurs, for so different systems like Ni + Pb and U + U, always after the net transfer of about 5% of the total number of nucleons. Also the three TKEL values from Xe + Pb indicate a similar trend. The evolution of the nuclear shapes shown in Fig. 1 (c) exhibits a somewhat steeper increase of the deformation at the beginning of the reaction, while in total the slope of the curves is more uniform than in TKEL (a) and interaction times (b). This indicates that the shape evolution proceeds more uniformly with increasing nucleon transfer than TKEL and the interaction time.

To understand the observed behavior, in the following, we investigate results of TDHF calculations and make a possible comparison with the experimental data. Nowadays it is feasible to systematically perform 3D TDHF calculations for various projectile-target combinations, impact parameters, and incident energies [23, 33, 34, 35, 36, 37, 38, 39], using a parallel computational code which works on hundreds of CPUs with MPI and OpenMP [39]. We show results for various systems, namely, ^{40}Ca+^{124}Sn ($E_{\mathrm{c.m.}} = 129$ MeV), ^{48}Ca+^{124}Sn ($E_{\mathrm{c.m.}} = 125$ MeV), ^{40}Ca+^{208}Pb ($E_{\mathrm{c.m.}} = 209$ MeV), ^{58}Ni+^{208}Pb ($E_{\mathrm{c.m.}} = 257$ MeV) [33], ^{64}Ni+^{238}U ($E_{\mathrm{c.m.}} = 307$ MeV) [23], ^{136}Xe+^{198}Pt ($E_{\mathrm{c.m.}} = 484$ MeV) [39], ^{40}Ar+^{208}Pb ($E_{\mathrm{c.m.}} = 218$ MeV), and ^{238}U+^{238}U ($E_{\mathrm{c.m.}} = 875$ MeV). For all results presented here, Skyrme SLy5 parameter set [40] was used for the EDF. TDHF calculations were performed for various impact parameters, typically 0–10 fm, for a given incident energy (except for ^{238}U+^{238}U, see below). For the ^{64}Ni+^{238}U reaction, three initial orientations of deformed ^{238}U (prolate, $\beta \simeq 0.27$) were investi-

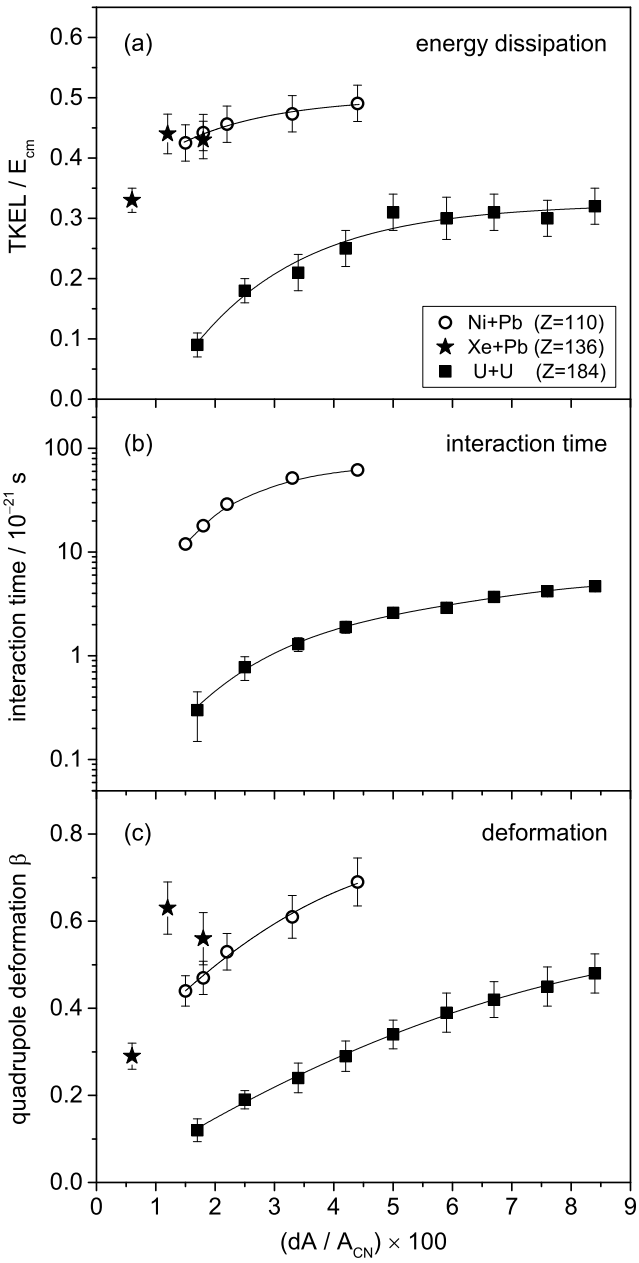

Fig. 1. Measured behavior of total kinetic energy loss (TKEL) (a), interaction times (b) and deformation of the fragments at the scission point (c) for collisions of ^{64}Ni+^{207}Pb ($E_{\mathrm{c.m.}} = 289$ MeV), ^{132}Xe+^{208}Pb ($E_{\mathrm{c.m.}} = 492$ MeV), and ^{238}U+^{238}U ($E_{\mathrm{c.m.}} = 875$ MeV) as a function of the fraction of transferred nucleons $\mathrm{d}A/A_{\mathrm{CN}}$.

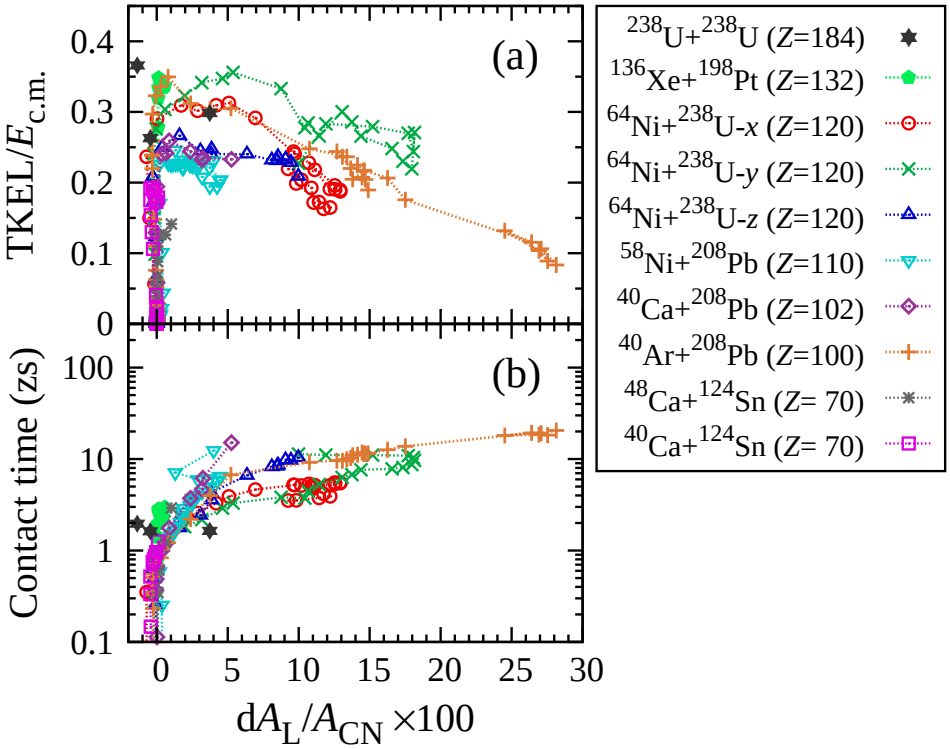

Fig. 2. Results of the TDHF calculations for various systems: ^{40}Ca+^{124}Sn (1.10), ^{48}Ca+^{124}Sn (1.09), ^{40}Ca+^{208}Pb (1.10), ^{40}Ar+^{208}Pb (1.37), ^{58}Ni+^{208}Pb (1.04), ^{64}Ni+^{238}U (x: 1.27, y and z: 1.16), ^{136}Xe+^{198}Pt (1.19), and ^{238}U+^{238}U (tip-on-tip: 1.32, tip-on-side: 1.23, side-on-side: 1.13) (The values in the parentheses are the ratio of center-of-mass energy to the frozen HF barrier height, $E_{\rm c.m.}/V_{\rm B}$). Total kinetic energy loss (TKEL) (a) and contact time (b) are shown. The horizontal axis is the change in the mass number of the lighter nucleus relative to the total number of nucleons in the composite system, $dA_L/A_{\rm CN}$. In panel (b), the contact time is shown in zeptosecond (1 zs = 10^{-21} sec).

gated, where the symmetry axis of ^{238}U was set parallel to the collision axis (x axis), impact parameter vector (y axis), or perpendicular to the reaction plane (parallel to z axis) [23]. For axially symmetric nuclei with a relatively small deformation [^{40}Ar (oblate, $\beta\simeq0.13$), ^{58}Ni (prolate, $\beta\simeq0.11$), ^{64}Ni (oblate, $\beta\simeq0.12$), ^{124}Sn (oblate, $\beta\simeq0.11$), and ^{136}Xe (oblate, $\beta\simeq0.06$)[2]], their symmetry axis was always set perpendicular to the reaction plane. For ^{198}Pt with a triaxial deformation ($\beta\simeq0.12$ with $\gamma\simeq33°$), the axis around

[2] The state of ^{136}Xe that was used for TDHF calculations turned out to be of a local minimum with 40 keV higher energy than the HF ground state (triaxial, $\beta\simeq0.06$ with $\gamma\simeq29°$). We note that no significant change is expected with this small deformation.

which $|Q_{22}|$ takes the smallest value is set perpendicular to the reaction plane. In reactions involving open shell nuclei, pairing correlations may play an important role. We note, however, that we ignore the pairing effects in the present article, as it requires additional computational effort.

First, we discuss the reaction mechanisms suggested by the TDHF calculations for various systems. In Fig. 2, TKEL, divided by the center-of-mass energy $E_{\rm c.m.}$, and contact time obtained from the TDHF calculations are shown in panels (a) and (b), respectively. The horizontal axis is the change in the mass number of the lighter nucleus, $\mathrm{d}A_L = \langle A_L \rangle - A_L$, divided by $A_{\rm CN}$, where $\langle A_L \rangle$ is the average mass number of the lighter fragment. TKEL was evaluated from the center-of-mass motion of the fragments [33]. The contact time is defined as the time duration during which the lowest density between two colliding nuclei exceeds a half of the nuclear saturation density, 0.08 fm^{-3} [23].

Let us first focus on the cases where the average number of transferred nucleons is small, a few percent of the total number of nucleons of the system. They correspond to (quasi)elastic and grazing reactions. In Fig. 2, the TDHF results exhibit a prominent increase of TKEL up to 20–35% of $E_{\rm c.m.}$ and of contact time up to about 1 zs. This trend is common for all systems examined here. After the rapid increase, TKEL is saturated, meaning that the available energy is fully transferred from the relative motion to internal degrees of freedom. Note that for ^{40,48}Ca+^{124}Sn (purple squares and gray asterisks) with a relatively small charge product ($Z_{\rm P}Z_{\rm T} = 1000$) the results end before the TKEL saturation since the system fused easily at smaller impact parameters. The TDHF results indicate that full energy dissipation is quickly achieved at the first stage of the reaction.

Next let us look at the cases where the average number of transferred nucleons is greater than a few percent of the total number of nucleons of the system. They correspond to trajectories at smaller impact parameters. In such cases, a dinuclear system connected with a thick neck is formed in the course of the collision and its shape evolution dynamics is responsible for the amount of nucleon transfer. As the impact parameter decreases, two nuclei collide more deeply, forming a more compact system connected with a thicker neck. It makes the contact time longer and the system evolves more towards the mass symmetry. It results in the behavior shown in Fig. 2 (b) that indicates a correlation between the amount of mass transfer and the contact time. In addition, Fig. 2 (a) shows a tendency that the TKEL decreases as the number of transferred nucleons increases ($\mathrm{d}A_L/A_{\rm CN} \gtrsim 10\%$). This is due to the fact that a larger mass transfer means also a larger proton transfer in this QF regime. As the number of transferred protons increases, the charge product of the fragments increases, which results in larger kinetic energy and, thus, smaller TKEL. The TDHF results indicate that, in

the second stage of the reaction, a large number of nucleons are collectively transferred via shape (mean-field) evolution dynamics in the composite system.

It is worth noting here similarities and differences of the TDHF results for different systems. In Fig. 2 (a), it is shown that the saturated values of TKEL for ^{40}Ca+^{208}Pb, ^{58}Ni+^{208}Pb, and ^{64}Ni+^{238}U (z-direction, blue open triangles) are very similar to each other, about 25% of $E_{\rm c.m.}$. On the other hand, the TKEL saturates at larger values, about 30–35% of $E_{\rm c.m.}$, for ^{40}Ar+^{208}Pb, ^{136}Xe+^{198}Pt, and ^{64}Ni+^{238}U (x- and y-direction, red circles and green crosses) reactions. In the latter case, the significance of nuclear orientations has been pointed out [23]. We note that the y-direction case (close to side collisions) results in larger energy dissipation compared with the x-direction case (close to tip collisions), for which one may expect the opposite trend since the barrier height is higher in the side collisions. Significant roles of the shape evolution dynamics and shell effects of ^{208}Pb in those damped collisions were extensively discussed in Ref. [23]. In the ^{40}Ar+^{208}Pb and ^{136}Xe+^{198}Pt reactions, the situation is somewhat different. In this case, the collision energy is larger compared with the other cases ($E_{\rm c.m.}/V_{\rm B} \simeq 1.37$ and 1.19, respectively). Because of this fact, a larger amount of energy is brought into the system that leads to a larger maximum value of TKEL (note also that in the ^{136}Xe+^{198}Pt reaction no fusion reaction was observed and larger TKEL is achieved at smaller impact parameters). Moreover, we observed several fusion-fission like processes in the ^{40}Ar+^{208}Pb reaction where the composite system splits in an almost symmetric way after a long contact time ($\approx$ 20 zs) which resulted in $\mathrm{d}A_L/A_{\rm CN} \simeq 28$ in Fig. 2, because of the large angular momentum brought into the system.

Here, let us make a possible comparison between the TDHF results and the experimental data. As mentioned above, the TDHF results correspond to contributions from main (most probable) trajectories with various scattering angles associated with different impact parameters. Whereas the experimental data shown in Fig. 1 were obtained by measurements for a fixed angular range: $\theta_{\rm lab} = (0 \pm 2)$ degrees (for Ni + Pb and Xe + Pb) and (35 ± 5) degrees (for U + U). Therefore, we should pay particular attention in comparing with the experimental data.

In the experiments on Ni + Pb [8] and Xe + Pb [9] at the velocity filter SHIP at GSI, only very central collisions were selectively detected, because of the angular acceptance of (0 ± 2) degrees. In central collisions, two nuclei must collide deeply forming a dinuclear system. In such a case, full energy dissipation should be achieved according to the TDHF results, as is also apparent from the long interaction time ($>$ 10 zs) (cf. Fig. 1 (b)). As shown in Fig. 1 (a), the experimental data exhibit almost saturated values of

TKEL, and thus, consistent with the TDHF results. Comparing the TDHF results for ^{58}Ni+^{208}Pb with the experimental data for ^{64}Ni+^{207}Pb, we find different TKEL values at saturation: in the former case it is about 25% of $E_{\rm c.m.}$, while in the latter case it is about 45–50% of $E_{\rm c.m.}$. This difference should arise from the different beam energies. In ^{58}Ni+^{208}Pb the energy was $E_{\rm c.m.}/V_{\rm Bass} \simeq 0.97$, while in ^{64}Ni+^{207}Pb it was $E_{\rm c.m.}/V_{\rm Bass} \simeq 1.11$, where $V_{\rm Bass}$ is the phenomenological fusion barrier [41]. One may notice here that, in the Xe + Pb case at $\mathrm{d}A/A_{\rm CN} < 1\%$ (Fig. 1 (a)), a noticeably small value of TKEL was deduced. It may be related to shell effects of ^{208}Pb which hinder energy dissipation and also lead to a small deformation of the fragments, resulting in larger TKE (smaller TKEL) [23]. Although we have no experimental values for Ni + Pb below $\mathrm{d}A/A_{\rm CN} = 1.5\%$, one may expect the same behavior also for Ni + Pb, extrapolating the curve down to $\mathrm{d}A/A_{\rm CN} < 1\%$. We note that it should also be influenced by the entrance-channel N/Z asymmetry, $|N_{\rm P}/Z_{\rm P} - N_{\rm T}/Z_{\rm T}|$, which is 0.24 for ^{64}Ni+^{207}Pb and 0.09 for ^{132}Xe+^{208}Pb, *i.e.*, in the former case it may weaken the shell effects by the charge equilibration process [42].

On the other hand, the experiment on U + U at the VAMOS spectrometer at GANIL [10] was optimized for detecting fragments around the grazing angle, which is relevant to the TDHF results for various systems shown in Fig. 2 (we expect that the universal behavior observed for other systems will also hold for U + U). In Fig. 1 (a), the experimental data show a rapid increase of TKEL for $\mathrm{d}A/A_{\rm CN} < 5\%$, while it is almost saturated for larger mass transfers. This behavior agrees with the reaction mechanisms deduced by TDHF, where substantial energy dissipation takes place even with transfer of a small number of nucleons. Moreover, in Ref. [10] measurements were performed for several incident energies, and it was revealed that TKE of the fragments becomes almost energy independent as the number of transferred nucleons increases, $\mathrm{d}A/A_{\rm CN} \gtrsim 3\%$. It is consistent with the observation in TDHF where full energy dissipation is quickly achieved and a large number of nucleons are transferred via the shape evolution dynamics in the composite system.

The experimental data shown in Fig. 1 (b) indicate that a remarkable time delay (up to around 4 zs) may still occur even for the heaviest accessible system U + U. The interaction time was deduced from the measured variance of the fragment masses σ_A^2 [10] assuming the relation $\sigma_A^2 = 2D_A\tau$, given by a diffusion model [43], where D_A is the mass diffusion coefficient (6.0×10^{22} s^{-1} for this reaction [10]) and τ is the interaction time. In order to investigate reaction mechanisms further, we performed exploratory TDHF calculations for head-on collisions of ^{238}U+^{238}U at $E_{\rm c.m.} = 875$ MeV with three configurations, *i.e.*, tip-on-tip, tip-on-side, and side-on-side collisions, where in the side-on-side configuration the symmetry axes of two ^{238}U were

aligned. The results are shown in Fig. 2 by black stars.

In the experiment [10], it has been clarified that more than 90% of the deep inelastic fragments resulted from $\tau < 2$ zs. From the TDHF calculations, we have obtained the contact times of 1.97 zs (tip-on-tip), 1.64 zs (tip-on-side), and 1.62 zs (side-on-side), which are consistent with the experimental observation. Although the contact time is rather short, substantial energy dissipation takes place. The values of TKEL/$E_{\rm c.m.}$ are 0.37 (tip-on-tip), 0.30 (tip-on-side), and 0.26 (side-on-side), which are again consistent with the experimental values shown in Fig. 1 (a).

One may notice that, even in this symmetric system, reaction products can be different from ^{238}U. The reason is two-fold. One is due to the broken reflection symmetry in the tip-on-side collision, which allows the system to split in an asymmetric way. In this process, about 11.2 neutrons and 6.6 protons are transferred on average from tip-aligned ^{238}U to the other, consistent with earlier studies [44, 45]. The other reason is due to a ternary QF process observed in the tip-on-tip collision. In the latter case, an extremely long (more than 10 fm) neck is developed when the system evolves towards the reseparation. The long neck becomes thinner at two points and eventually raptures producing a small third fragment in between two heavy nuclei. We observed a beryllium-like nucleus ($Z \simeq 4.1$, $N \simeq 6.5$) as the third fragment. The formation of ternary fragments in tip-on-tip collisions of ^{238}U+^{238}U was also reported in Ref. [44]. In this way, TDHF predicts significant impacts of nuclear orientations on the fragment masses in collisions of two well-deformed actinide nuclei.

Finally, we investigate the variance of the fragment masses σ_A^2 in the ^{238}U+^{238}U reaction. Although TDHF provides a fairly good description for averaged quantities, it substantially underestimates the variance of the fragment masses. Thus one has to go beyond the standard mean-field description [46, 47, 48, 49]. Here, we examine the variance employing the Balian-Véneroni (BV) variational principle [47] which enables to include fluctuations and correlations around the mean-field trajectory. For tip-on-side and side-on-side collisions, where we observed binary reaction products[3], the BV prescription gives $\sigma_A^2 \simeq 236.4$ and 148.2, respectively, which are significantly larger than those by TDHF, $\sigma_A^2 \simeq 10.5$ and 9.6. For the tip-on-side and side-on-side collisions, we have TKEL values of 263 and 224 MeV, respectively, and experimental values corresponding to those TKEL values are $\sigma_A^2 \approx 400$ and 250 (cf. Fig. 13 of Ref. [10]). Although this is a crude comparison, as calculations were performed only for head-on collisions and the experimental variance is very sensitive to TKEL values, one can see that remarkable improvement is achieved by the BV prescription. We note that the experi-

[3] For tip-on-tip collision, where we observed the ternary QF process, the BV prescription provided an unphysically large value of the variance (not shown).

mental data may be influenced by the orientation dependence, as deduced by TDHF calculations, as well as secondary processes (particle evaporation and fission), which may increase the variance of the fragment masses, σ_A^2.

5. Summary and perspective

We have performed theoretical and experimental studies on the stability of heavy and superheavy nuclear systems with total proton numbers up to $Z = 184$ by investigating nuclear molecule formation and time delays in deep-inelastic binary reactions at energies around the Coulomb barrier.

The experimental data for ^{64}Ni+^{207}Pb ($E_{\rm c.m.} = 289$ MeV) [8], ^{132}Xe+^{208}Pb ($E_{\rm c.m.} = 492$ MeV) [9], and ^{238}U+^{238}U ($E_{\rm c.m.} = 875$ MeV) [10] show striking similarities in the behavior of energy dissipation, interaction times, and deformation of the fragment nuclei. In the first stage of the reaction, where the amount of nucleon transfer is less than 5% of the total number of nucleons in the composite system, a lot of time is spent to move only a small number of nucleons and large energy is transferred into internal excitations. In the second stage, the interaction time increases slowly even if a large number of nucleons are transferred. The observed similarities indicate that a significant time delay may still occur even in the heaviest accessible system U + U.

To understand the observed behavior, we have carried out a comparative study between results of TDHF calculations for various systems [^{40}Ca+^{124}Sn ($E_{\rm c.m.} = 129$ MeV), ^{48}Ca+^{124}Sn ($E_{\rm c.m.} = 125$ MeV), ^{40}Ca+^{208}Pb ($E_{\rm c.m.} = 209$ MeV), ^{40}Ar+^{208}Pb ($E_{\rm c.m.} = 218$ MeV), ^{58}Ni+^{208}Pb ($E_{\rm c.m.} = 257$ MeV), ^{64}Ni+^{238}U ($E_{\rm c.m.} = 307$ MeV), ^{136}Xe+^{198}Pt ($E_{\rm c.m.} = 484$ MeV), and ^{238}U+^{238}U ($E_{\rm c.m.} = 875$ MeV)] and the experimental data. From the results of the TDHF calculations for different systems, we have found similar trends as observed in the experimental data.

The TDHF results have revealed occurrence of two distinct transfer mechanisms. In the grazing regime, a small number of nucleons are transferred through a fast charge equilibration process. At this stage substantial energy dissipation (TKEL/$E_{\rm c.m.} \approx 20$–35%) takes place in a relatively short period (about 1–2 zs) and available kinetic energy is fully dissipated. This represents a rapid transition from quasi-elastic to deep-inelastic and QF regimes. As the impact parameter decreases, two nuclei collide more deeply forming a dinuclear system connected with a thick neck. In the latter case shape evolution dynamics of the composite system is responsible for the amount of nucleon transfer. A large number of nucleons are effectively transferred via the shape evolution dynamics, while all kinetic energy is already fully dissipated.

TDHF calculations were also performed for head-on collisions of ^{238}U+

^{238}U ($E_{\mathrm{c.m.}} = 875$ MeV) with three orientations, *i.e.*, tip-on-tip, tip-on-side, and side-on-side collisions. The results of TKEL and contact time are in reasonable agreement with the experimental data. In the tip-on-tip collision, we have observed a ternary QF process, where a small third fragment is generated from the neck region between two heavy nuclei. In the tip-on-side collision, the broken reflection symmetry allows the composite system to split in an asymmetric way, resulting in transfer of many nucleons from tip-aligned ^{238}U to the other. Moreover, the Balian-Vénéroni variational principle was applied to investigate the variance of the fragment masses in the U + U system, showing significant improvement compared with TDHF.

A careful observation of the experimental data revealed striking similarities between Ni + Pb and U + U systems that the slope change of TKEL and interaction times occurs always after the net transfer of about 5% of the total number of nucleons. We could not yet draw a conclusion if a physical meaning is behind or it is just by chance. We consider that further analyses of different reactions measured at SHIP or VAMOS will provide useful information, which we leave as a future task.

It has been shown that the microscopic TDHF theory can be a promising tool to investigate the QF dynamics in heavy and superheavy systems. The theory provides valuable insight into the complex QF dynamics from nucleonic degrees of freedom, thus, taking into account shell effects during the collision process. Recently, it has been suggested, based on the Langevin model, that multinucleon transfer and QF processes are useful to produce neutron-rich (super)heavy nuclei which have not been produced to date, where shell effects are predicted to play an important role (see, *e.g.*, [50]). In principle, TDHF can also describe the predicted shell-effect driven transfer processes, and an extensive analysis is in progress [51].

Last but not least, there is an open problem that how and to what extent the pairing correlations affect the reaction dynamics in damped collisions of heavy nuclei. The so-called time-dependent superfluid local density approximation (TDSLDA) (or time-dependent Hartree-Fock-Bogoliubov theory, TDHFB) would provide a satisfactory answer to it, although it requires about 100–1000 times larger computational cost compared with that for the TDHF calculation. Very recently, it has become possible to perform 3D TDSLDA calculations for nuclear systems using leadership-class supercomputers with hundreds of GPUs [52, 53, 54, 55, 56]. On one hand, pairing effects should disappear as the excitation energy increases, on the other hand the additional degrees of freedom associated with complex pairing field dynamics may still alter the QF timescale in a similar way as observed in ^{240}Pu induced fission process [54]. A study along this line is in progress [57], and the results will be published elsewhere.

Acknowledgments

K.S. acknowledges support of Polish National Science Centre (NCN) Grant, decision No. DEC-2013/08/A/ST3/00708. The numerical calculations were performed using computational resources of the HPCI system (HITACHI SR16000/M1) provided by Information Initiative Center, Hokkaido University, through the HPCI System Research Projects (Project IDs: hp120204, hp140010, hp150081, and hp160062), and using computational resources of the Cray XC40 supercomputer system at the Yukawa Institute for Theoretical Physics (YITP) at Kyoto University.

REFERENCES

[1] W. Greiner, J.Y. Park, and W. Scheid, *Nuclear Molecules* (World Scientific, 1995).

[2] V.V. Volkov, Phys. Rep. **44**, 93 (1978).

[3] R. Bock, Y.T. Chu, M. Dakowski, A. Gobbi, E. Grosse, A. Olmi, H. Sann, D. Schwalm, U. Lynen, W. Müller, S. Bjørnholm, H. Esbensen, W. Wölfli, and E. Morenzoni, Nucl. Phys. **A388**, 334 (1982).

[4] J. Tōke, R. Bock, G.X. Dai, A. Gobbi, S. Gralla, K.D. Hildenbrand, J. Kuzminski, W.F.J. Müller, A. Olmi, H. Stelzer, B.B. Back, and S. Bjørnholm, Nucl. Phys. **A440**, 327 (1985).

[5] W.Q. Shen, J. Albinski, A. Gobbi, S. Gralla, K.D. Hildenbrand, N. Herrmann, J. Kuzminski, W.F.J. Müller, H. Stelzer, J. Tke, B.B. Back, S. Bjrnholm, and S.P. Srensen, Phys. Rev. C **36**, 115 (1987).

[6] R. du Rietz, D.J. Hinde, M. Dasgupta, R.G. Thomas, L.R. Gasques, M. Evers, N. Lobanov, and A. Wakhle, Phys. Rev. Lett. **106**, 052701 (2011).

[7] R. du Rietz, E. Williams, D.J. Hinde, M. Dasgupta, M. Evers, C.J. Lin, D.H. Luong, C. Simenel, and A. Wakhle, Phys. Rev. C **88**, 054618 (2013).

[8] V. Comas, S. Heinz, S. Hofmann, D. Ackermann, J. Heredia, F.P. Heßberger, J. Khuyagbaatar, B. Kindler, B. Lommel, and R. Mann, Eur. Phys. J. A **48**, 180 (2012).

[9] S. Heinz, O. Beliuskina, V. Comas, H.M. Devaraja, C. Heinz, S. Hofmann, E. Kozulin, F. Morherr, G. Münzenberg, D. Ackermann, F.P. Heßberger, B. Kindler, B. Lommel, R. Mann, and J. Maurer, Eur. Phys. J. A **51**, 140 (2015).

[10] C. Golabek, S. Heinz, W. Mittig, F. Rejmund, A.C.C. Villari, S. Bhattacharyva, D. Boilley, G. De France, A. Drouart, L. Gaudefroy, L. Giot, V. Maslov, M. Morjean, G. Mukherjee, Yu. Penionzkevich, P. Roussel-Chomaz, and C. Stodel, Eur. Phys. J. A **43**, 251 (2010).

[11] V. Zagrebaev and W. Greiner, J. Phys. G: Nucl. Part. Phys. **31**, 825 (2005).

[12] V. Zagrebaev and W. Greiner, J. Phys. G: Nucl. Part. Phys. **34**, 1 (2007).

[13] G.G Adamian, N.V. Antonenko, and W. Scheid, Nucl. Phys. **A618**, 176 (1997).

[14] G.G Adamian, N.V. Antonenko, W. Scheid, and V.V. Volkov, Nucl. Phys. **A627**, 361 (1997).

[15] L. Zhu, Z.-Q. Feng, and F. S. Zhang, J. Phys. G: Nucl. Part. Phys. **42**, 085102 (2015).

[16] M.-H. Mun, G.G. Adamian, N.V. Antonenko, Y. Oh, and Y. Kim, Phys. Rev. C **91**, 054610 (2015).

[17] N. Wang, Z. Li, and X. Wu, Phys. Rev. C **65**, 064608 (2002).

[18] N. Wang, Z. Li, X. Wu, J. Tian, Y. Zhang, and M. Liu, Phys. Rev. C **69**, 034608 (2004).

[19] K. Zhao, Z. Li, N. Wang, Y. Zhang, Q. Li, Y. Wang, and X. Wu, Phys. Rev. C **92**, 024613 (2015).

[20] K. Zhao, Z. Li, Y. Zhang, N. Wang, Q. Li, C. Shen, Y. Wang, and X. Wu, Phys. Rev. C **94**, 024601 (2016).

[21] J.W. Negele, Rev. Mod. Phys. **54**, 913 (1982).

[22] C. Simenel, Eur. Phys. J. A **48**, 152 (2012).

[23] K. Sekizawa and K. Yabana, Phys. Rev. C **93**, 054616 (2016).

[24] A.S. Umar, V.E. Oberacker, and C. Simenel, Phys. Rev. C **94**, 024605 (2016).

[25] A. Wakhle, C. Simenel, D.J. Hinde, M. Dasgupta, M. Evers, D.H. Luong, R. du Rietz, and E. Williams, Phys. Rev. Lett. **113**, 182502 (2014).

[26] V.E. Oberacker, A.S. Umar, and C. Simenel, Phys. Rev. C **90**, 054605 (2014).

[27] K. Washiyama, Phys. Rev. C **91**, 064607 (2015).

[28] K. Hammerton, Z. Kohley, D.J. Hinde, M. Dasgupta, A. Wakhle, E. Williams, V.E. Oberacker, A.S. Umar, I.P. Carter, K.J. Cook, J. Greene, D.Y. Jeung, D.H. Luong, S.D. McNeil, C.S. Palshetkar, D.C. Rafferty, C. Simenel, and K. Stiefel, Phys. Rev. C **91**, 041602(R) (2015).

[29] A.S. Umar, V.E. Oberacker, and C. Simenel, Phys. Rev. C **92**, 024621 (2015).

[30] S. Hofmann and G. Münzenberg, Rev. Mod. Phys. **72**, 733 (2000).

[31] H. Savajols, Nucl. Instrum. Methods B **204**, 146 (2003).

[32] S. Hofmann, F.P. Heßberger, D. Ackermann, S. Antalic, P. Cagarda, S. Ćwiok, B. Kindler, I. Kojouharov, B. Lommel, R. Mann, G. Münzenberg, A.G. Popeko, S. Saro, H.J. Schött, and A.V. Yeremin, Eur. Phys. J. A **10**, 5 (2001).

[33] K. Sekizawa and K. Yabana, Phys. Rev. C **88**, 014614 (2013); **93**, 029902(E) (2016).

[34] K. Sekizawa and K. Yabana, Phys. Rev. C **90**, 064614 (2014).

[35] K. Sekizawa and K. Yabana, EPJ Web of Conf. **86**, 00043 (2015).

[36] K. Sekizawa and K. Yabana, JPS Conf. Proc. **6**, 030084 (2015).

[37] K. Sekizawa and K. Yabana, *Multinucleon transfer reaction in time-dependent Hartree-Fock theory*, an invited paper honoring Prof. Joachim Maruhn's retirement to be published as a chapter in "Progress of time-dependent nuclear reaction theory" (ed. Yoritaka Iwata) in the ebook series: "Frontiers in nuclear and particle physics" (Bentham Science Publishers); arXiv:1511.08322 [nucl-th].

[38] Sonika, B.J. Roy, A. Parmar, U.K. Pal, H. Kumawat, V. Jha, S.K. Pandit, V.V. Parkar, K. Ramachandran, K. Mahata, A. Pal, S. Santra, A.K. Mohanty, and K. Sekizawa, Phys. Rev. C **92**, 024603 (2015).

[39] K. Sekizawa, Multinucleon Transfer Reactions and Quasifission Processes in Time-Dependent Hartree-Fock Theory, Ph.D. thesis, University of Tsukuba, 2015.

[40] E. Chabanat, P. Bonche, P. Haensel, J. Meyer, and R. Schaeffer, Nucl. Phys. **A635**, 231 (1998); **A643**, 441 (1998).

[41] R. Bass, Nucl. Phys. **A231**, 45 (1974).

[42] C. Simenel, D.J. Hinde, R. du Rietz, M. Dasgupta, M. Evers, C.J. Lin, D.H. Luong, A. Wakhle, Phys. Lett. B **710**, 607 (2012).

[43] C. Riedel, G. Wolschin, and W. Nörenberg, Z. Phys. A **290**, 47 (1979).

[44] C. Golabek and C. Simenel, Phys. Rev. Lett. **103**, 042701 (2009).

[45] D.J. Kedziora and C. Simenel, Phys. Rev. C **81**, 044613 (2010).

[46] D. Lacroix, *Large amplitude collective dynamic beyond the independent particle/quasiparticle picture*, an invited paper honoring Prof. Joachim Maruhn's retirement to be published as a chapter in "Progress of time-dependent nuclear reaction theory" (ed. Yoritaka Iwata) in the ebook series: "Frontiers in nuclear and particle physics" (Bentham Science Publishers); arXiv:1504.01499 [nucl-th].

[47] C. Simenel, Phys. Rev. Lett. **106**, 112502 (2011).

[48] S. Ayik, B. Yilmaz, and O. Yilmaz, Phys. Rev. C **92**, 064615 (2015).

[49] M. Tohyama and A.S. Umar, Phys. Rev. C **93**, 034607 (2016).

[50] V. Zagrebaev and W. Greiner, J. Phys. G: Nucl. Part. Phys. **34**, 2265 (2007).

[51] K. Sekizawa, in preparation.

[52] I. Stetcu, A. Bulgac, P. Magierski, and K.J. Roche, Phys. Rev. Lett. **114**, 012701 (2015).

[53] P. Magierski, *Nuclear Reactions and Superfluid Time Dependent Density Functional Theory*, an invited paper honoring Prof. Joachim Maruhn's retirement to be published as a chapter in "Progress of time-dependent nuclear reaction theory" (ed. Yoritaka Iwata) in the ebook series: "Frontiers in nuclear and particle physics" (Bentham Science Publishers); arXiv:1606.02225 [nucl-th].

[54] A. Bulgac, P. Magierski, K.J. Roche, and I. Stetcu, Phys. Rev. Lett. **116**, 122504 (2016).

[55] G. Wlazłowski, K. Sekizawa, P. Magierski, A. Bulgac, and M.M. Forbes, Phys. Rev. Lett. **117**, 232701 (2016).

[56] K. Sekizawa, G. Wlazłowski, P. Magierski, A. Bulgac, and M.M. Forbes, JPS Conf. Proc. (in press); arXiv:1609.03865 [nucl-th].

[57] P. Magierski, K. Sekizawa, and G. Wlazłowski, arXiv:1611.10261 [nucl-th].